euronoise

Circumferential admittance approach for vibro-acoustic prediction of a submerged cylindrical shell with rib aperiodicity and transversal bulkheads

Laurent Maxit

DGA (Defence Agency), CTSN/SDP/CMPF, B.P. 28, 83800 Toulon, France
laurent.maxit@dga.defense.gouv.fr

The circumferential admittance approach is presented to predict the vibro-acoustic behaviour of an externally fluid loaded shell with aperiodic stiffeners and transversal bulkheads. It consists to consider the circumferential spectral displacements of the shell and to use a partitioning of the structure such that the fluid loaded shell constitutes one subsystem and the stiffeners/bulkheads constitute others subsystems. Each subsystem is characterised independently by the circumferential admittances. For the stiffeners/bulkheads, a standard FE code is used to calculate these admittances with a shell description. The admittances of the fluid load shell are estimated by a spectral approach. Developments are proposed in this paper to improve the numerical convergence of the spectral approach. The final assembly is obtained using the continuity relations. Excitations like mechanical forces, acoustic diffuse fields or plane waves can be easily taken into account. For submarine applications, this model permits to study the noise radiated by the pressure hull or to analyse the acoustic target strength of the shell with its internal frames. The whole submarine pressure hull can be described with the assumption that it is extended by a cylindrical rigid baffle. Numerical validations and results at several kHz are shown for a submarine application.

1 Introduction

The acoustic performances of a submarine hull intervene on different operational capacities of the submarine:
- the radiated noise in the far field influences the invulnerability performance of the submarine;
- the radiated noise in the near field (self noise) can reduce the Sonar performances;
- the acoustic wave reflection on the hull has a role again the active Sonar threat (target strength).

To improve the knowledge in this area, numerous scientists have developed models to analyse the vibro-acoustic behaviour of fluid loaded stiffened shell (see the recent works [1-8]). In order to be representative of the submarine pressure hull, the modelling should at least take into account:
- the cylindrical hull and its interaction with the external fluid (water);
- the bulkheads between the different compartments and the ends of the pressure hull;
- the stiffeners with a spacing which can vary along the shell.

In the literature, few attentions have been devoted to the modelling of the stiffeners: generally, beam behaviour is assumed in spite of a finite element model of a typical submarine stiffener can show, even at low frequency, a deformation of the cross section. The behaviour of the stiffeners may strongly influence the vibration of the shell and its acoustic radiation. An accurate modelling of the internal frames of the shell is then requested. This point will be especially address here. A submarine pressure hull model is developed in this paper by substructuring the vibro-acoustic problem using the Circumferential Admittance Approach (CAA). This approach permits to assemble an analytical model of the fluid loaded shell with finite element models of the internal frames. With this approach, calculations may be achieved in a large frequency band (until several kHz for a typical submarine pressure hull) and different types of excitations may be introduced: mechanical forces on the shell or the frames, internal diffuse field, external plane wave.

One describes this approach in the next section. Numerical validations and submarine application are shown in section 3 and 4, respectively.

2 Circumferential Admittance Approach

2.1 Principle

A ring-stiffened cylindrical shell immersed in water shown in Fig. 1 (a) is considered. The shell is characterized by a constant thickness h, a mean radius R, a mass density ρ, the Young's modulus E, and the Poisson ratio ν. The shell is supposed to have an infinite length but clamped boundary conditions are introduced to simulate the finite length of a submarine hull. The Θ internal frames are composed of different sorts of stiffeners, bulkheads and hemispherical endcaps. Theses frames are supposed axially symmetric and are located at the axial distance x_i, $i \in [1,\Theta]$. (r,θ,x) are the cylindrical coordinates as shown on Fig 1. To have a short presentation, the external load is supposed to be contain in the plane θ=0. It is however not a limitation of the technique.

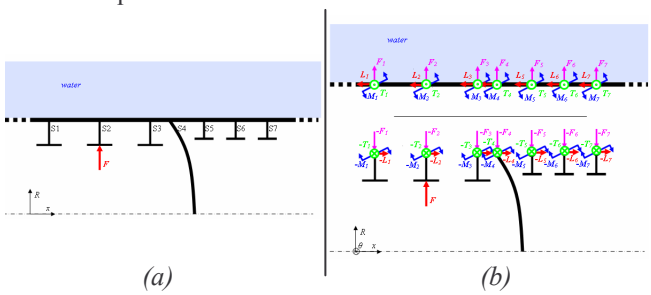

(a) (b)

Figure 1. (a), Fluid loaded stiffened shell; (b), Partitioning and coupling forces.

As shown on Fig. 1 (b), the structure is partitioned such that the fluid loaded shell constitutes one subsystem and the frames constitute others independent subsystems. One defines at the junction between shell and the i^{th} frame:

- $W_i^{\text{shell}}, U_i^{\text{shell}}, V_i^{\text{shell}}$ and φ_i^{shell} (resp. $W_i^{\text{frame}}, U_i^{\text{frame}}, V_i^{\text{frame}}$ and φ_i^{frame}) the radial displacement, the axial displacement, the circumferencial displacement, and the rotation ($\varphi = \partial W/\partial x$) of the shell (resp. the frame);

- $F_i^{\text{shell}}, L_i^{\text{shell}}, T_i^{\text{shell}}$ and M_i^{shell} (resp. $F_i^{\text{frame}}, L_i^{\text{frame}}, T_i^{\text{frame}}$ and M_i^{frame}) the radial force, the axial force, the circumferencial force, and the moment acting on the frame (resp. shell) by the shell (resp. frame).

The circumferential spectral of these quantities is defined by their Fourier transforms on θ:

$$\bullet(\theta) \xrightarrow{T.F.} \tilde{\bullet}(k_\theta) = \frac{1}{2\pi}\int_{-\infty}^{\infty} \bullet(\theta) e^{-jk_\theta\theta} d\theta \qquad (1)$$

where k_θ is the circumferential wave number.

Considering the symmetric plane θ=0 and the circumferential periodicity, one has the properties:

$$\begin{cases} \left|\tilde{\bullet}(-k_\theta)\right| = \left|\tilde{\bullet}(k_\theta)\right|, \\ \tilde{\bullet} = 0, \text{ if } k_\theta \notin Z. \end{cases} \qquad (2)$$

Then, in the following, calculations will be achieved for a given circumferential wave number equals the circumferential order, n with $n \in N$. This circumferential wave number will be omitted in the notation.

One defines:

- the circumferential admittances of the shell (resp. frame) between the i^{th} junction and the j^{th} junction, $\tilde{Y}^{\text{shell}}_{\xi_i\zeta_j}$ (resp. $\tilde{Y}^{\text{frame}}_{\xi_i\zeta_j}$) by:

$$\tilde{Y}^{\text{shell}}_{\xi_i\zeta_j} = \frac{\tilde{\xi}^{\text{shell}}_i}{\tilde{\zeta}^{\text{shell}}_i} \text{ (resp. } \tilde{Y}^{\text{frame}}_{\xi_i\zeta_j} = \frac{\tilde{\xi}^{\text{frame}}_i}{\tilde{\zeta}^{\text{frame}}_i}\text{)}, \qquad (3)$$

where $\xi \in \{W, U, V, \varphi\}$ and $\zeta \in \{F, L, T, M\}$;

- the free circumferential displacement of the shell, $\bar{\tilde{\xi}}^{\text{shell}}_i$ (resp. frame, $\bar{\tilde{\xi}}^{\text{frame}}_i$) as the circumferential displacements of the uncoupled shell (resp. frame) excited by the external load.

These circumferential admittances and free displacements are evaluated independently each other. One can note that for an external force on the I^{th} frame, all the free circumferential displacements are null excepted for the I^{th} frame:

$$\begin{cases} \bar{\tilde{\xi}}^{\text{shell}}_i = 0, \forall i \in [1, \Theta]; \\ \bar{\tilde{\xi}}^{\text{frame}}_i = 0, \forall i \in \{[1, \Theta] / i \neq I\}; \bar{\tilde{\xi}}^{\text{frame}}_I = \hat{\tilde{\xi}}. \end{cases} \qquad (4)$$

Using the superposition principle for linear passive system, the displacements continuity and equilibrium conditions at the junctions between the shell and the frames, one can write:

$$\begin{cases} \sum_{j=1}^{\Theta} \left[\left(\tilde{Y}^{\text{shell}}_{W_iF_j} + \tilde{Y}^{\text{frame}}_{W_iF_j}\right)\tilde{F}^{\text{frame}}_j + \left(\tilde{Y}^{\text{shell}}_{W_iM_j} + \tilde{Y}^{\text{frame}}_{W_iM_j}\right)\tilde{M}^{\text{frame}}_j \right. \\ \left. + \left(\tilde{Y}^{\text{shell}}_{W_iL_j} + \tilde{Y}^{\text{frame}}_{W_iL_j}\right)\tilde{L}^{\text{frame}}_j + \left(\tilde{Y}^{\text{shell}}_{W_iT_j} + \tilde{Y}^{\text{frame}}_{W_iT_j}\right)\tilde{T}^{\text{frame}}_j \right] = \bar{\tilde{W}}^{\text{frame}}_i - \bar{\tilde{W}}^{\text{shell}}_i, \\ \sum_{j=1}^{\Theta} \left[\left(\tilde{Y}^{\text{shell}}_{\varphi_iF_j} + \tilde{Y}^{\text{frame}}_{\varphi_iF_j}\right)\tilde{F}^{\text{frame}}_j + \left(\tilde{Y}^{\text{shell}}_{\varphi_iM_j} + \tilde{Y}^{\text{frame}}_{\varphi_iM_j}\right)\tilde{M}^{\text{frame}}_j \right. \\ \left. + \left(\tilde{Y}^{\text{shell}}_{\varphi_iL_j} + \tilde{Y}^{\text{frame}}_{\varphi_iL_j}\right)\tilde{L}^{\text{frame}}_j + \left(\tilde{Y}^{\text{shell}}_{\varphi_iT_j} + \tilde{Y}^{\text{frame}}_{\varphi_iT_j}\right)\tilde{T}^{\text{frame}}_j \right] = \bar{\tilde{\varphi}}^{\text{frame}}_i - \bar{\tilde{\varphi}}^{\text{shell}}_i, \\ \sum_{j=1}^{\Theta} \left[\left(\tilde{Y}^{\text{shell}}_{U_iF_j} + \tilde{Y}^{\text{frame}}_{U_iF_j}\right)\tilde{F}^{\text{frame}}_j + \left(\tilde{Y}^{\text{shell}}_{U_iM_j} + \tilde{Y}^{\text{frame}}_{U_iM_j}\right)\tilde{M}^{\text{frame}}_j \right. \\ \left. + \left(\tilde{Y}^{\text{shell}}_{U_iL_j} + \tilde{Y}^{\text{frame}}_{U_iL_j}\right)\tilde{L}^{\text{frame}}_j + \left(\tilde{Y}^{\text{shell}}_{U_iT_j} + \tilde{Y}^{\text{frame}}_{U_iT_j}\right)\tilde{T}^{\text{frame}}_j \right] = \bar{\tilde{U}}^{\text{frame}}_i - \bar{\tilde{U}}^{\text{shell}}_i, \\ \sum_{j=1}^{\Theta} \left[\left(\tilde{Y}^{\text{shell}}_{V_iF_j} + \tilde{Y}^{\text{frame}}_{V_iF_j}\right)\tilde{F}^{\text{frame}}_j + \left(\tilde{Y}^{\text{shell}}_{V_iM_j} + \tilde{Y}^{\text{frame}}_{V_iM_j}\right)\tilde{M}^{\text{frame}}_j \right. \\ \left. + \left(\tilde{Y}^{\text{shell}}_{V_iL_j} + \tilde{Y}^{\text{frame}}_{V_iL_j}\right)\tilde{L}^{\text{frame}}_j + \left(\tilde{Y}^{\text{shell}}_{V_iT_j} + \tilde{Y}^{\text{frame}}_{V_iT_j}\right)\tilde{T}^{\text{frame}}_j \right] = \bar{\tilde{V}}^{\text{frame}}_i - \bar{\tilde{V}}^{\text{shell}}_i, \\ \qquad \forall i \in [1, \Theta] \end{cases} \qquad (5)$$

This equation system may be written on the compact matrix form:

$$\left[\tilde{\mathbf{Y}}^{\text{shell}} + \tilde{\mathbf{Y}}^{\text{frame}}\right]\left[\tilde{\mathbf{F}}^{\text{frame}}\right] = \left[\bar{\tilde{\mathbf{W}}}^{\text{frame}} - \bar{\tilde{\mathbf{W}}}^{\text{shell}}\right]. \qquad (6)$$

By solving it, one deduces the forces and the moments of the frames acting on the shell when they are coupled together.

One describes the process to estimate: $\tilde{\mathbf{Y}}^{\text{frame}}$, $\bar{\tilde{\mathbf{W}}}^{\text{frame}}$ in section 2.2; $\tilde{\mathbf{Y}}^{\text{shell}}$, $\bar{\tilde{\mathbf{W}}}^{\text{shell}}$ in section 2.3, and; the vibration and the radiated pressure from the shell coupled with its internal frames from $\tilde{\mathbf{F}}^{\text{frame}}$ in section 2.4.

2.2 Frames

Axisymmetric Finite Elements and MSC/NASTRAN code are used to estimate the circumferential admittances and free displacements of each type of frames (stiffeners/bulkheads/endcaps). The conical shell elements CCONEAX with the PCONEAX properties permit to describe the frame behaviour from a mesh of the cross section. Complex geometry of the cross section can be described and thickness variations may be taken into account easily. Calculations are achieved for harmonic orders of Fourier series which are equivalent to the circumferential orders of the present paper. Displacements at the junction are evaluated for different load directions using a direct analysis (SOL. 108). Pre and post-processing are achieved from a MATLAB code. One can notice that these calculations are necessary for each type of frame, and not for all the frames.

Remark: the clamped boundary conditions at the ends of the cylindrical shell are introduced by considering a frame with null circumferential admittances.

Finite Elements results are proposed on the next two figures. Fig. 2 illustrates the deformation of the cross section of this considered stiffener, which is contrary to the classical beam assumption. Fig. 3 compares the circumferential admittances Y_{WF} and $Y_{\theta M}$ calculated with NASTRAN and with the beam assumptions.

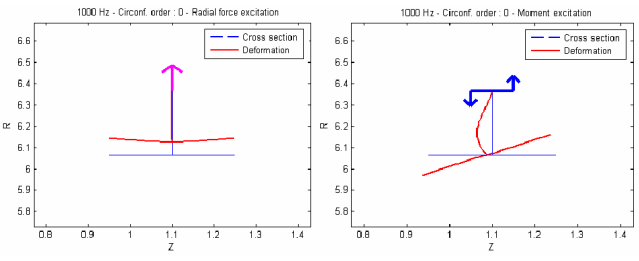

(a) *(b)*

Figure 2. Deformation of a stiffener cross section: (a), radial force excitation; (b), moment excitation. 1000 Hz, n=0. T section: 300mm x 60mm / 60mm x 300mm. Material: steel.

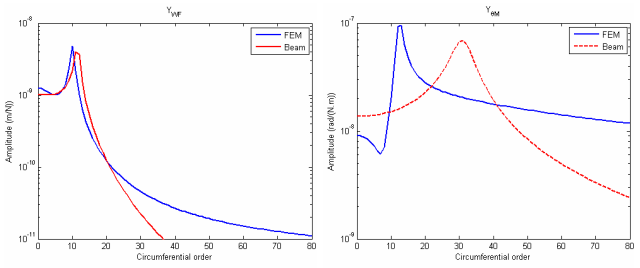

(a) *(b)*

Figure 3. Comparison of the circumferential admittances calculated with NASTRAN and with the beam assumptions: (a), Y_{WF} ; (b), $Y_{\theta M}$.

2.3 Fluid loaded shell

2.3.1 Principle of the wave-number approach

Consider the infinite cylindrical shell immersed in fluid and excited by mechanical forces. The Flugge equations of motions [9] describe the dynamic behaviour of this shell. In the second member, the external forces and the parietal pressure appear. The resolution of this problem by the wave-number approach consists to apply a space-Fourier transform at these equations. This transform yields:

$$\begin{bmatrix} \tilde{\tilde{Z}}_{UU} & \tilde{\tilde{Z}}_{UV} & \tilde{\tilde{Z}}_{UW} \\ \tilde{\tilde{Z}}_{UV} & \tilde{\tilde{Z}}_{VV} & \tilde{\tilde{Z}}_{VW} \\ \tilde{\tilde{Z}}_{UW} & \tilde{\tilde{Z}}_{VW} & \tilde{\tilde{Z}}_{WW} \end{bmatrix} \begin{bmatrix} \tilde{\tilde{U}} \\ \tilde{\tilde{V}} \\ \tilde{\tilde{W}} \end{bmatrix} = \frac{(1-\nu^2)}{Eh} \begin{bmatrix} -\tilde{\tilde{L}} \\ -\tilde{\tilde{T}} \\ \tilde{\tilde{F}} - \tilde{\tilde{p}} \end{bmatrix}, \qquad (7)$$

where :

- $\tilde{\tilde{\bullet}}(k_x, k_\theta)$ denotes the space Fourier transform of the quantity $\bullet(x,\theta)$;

- k_x is the axial wavenumber, and;

$$\tilde{\tilde{Z}}_{UU} = -R^2 {k_x}^2 - {k_\theta}^2 \frac{1-\nu}{2}(1+\beta^2) + R^2 {k_l}^2, \tilde{\tilde{Z}}_{UV} = -R\frac{1+\nu}{2} k_\theta k_x,$$

$$\tilde{\tilde{Z}}_{UW} = jk_x \left(R\nu + \beta^2 R^3 {k_x}^2 - \beta^2 R \frac{1-\nu}{2} {k_\theta}^2 \right),$$

$$\tilde{\tilde{Z}}_{VV} = -R^2 {k_x}^2 \frac{1-\nu}{2}(1+3\beta^2) - {k_\theta}^2 + R^2 {k_l}^2,$$

$$\tilde{\tilde{Z}}_{VW} = jk_\theta \left(1 + \beta^2 R^2 \frac{3-\nu}{2} {k_x}^2 \right),$$

$$\tilde{\tilde{Z}}_{WW} = 1 + \beta^2 \left[R^4 {k_x}^4 + {k_\theta}^2 (2R^2 {k_x}^2 + 2) + {k_\theta}^4 + 1 \right] - {k_l}^2,$$

$$\beta = \frac{h}{R\sqrt{12}}, k_l = \omega \sqrt{\frac{\rho(1-\nu^2)}{E}}. \qquad (8)$$

The spectral pressure $\tilde{\tilde{p}}$ may be evaluated by resolving the Helmholtz equation [10]:

$$\tilde{\tilde{p}} = \tilde{\tilde{Z}}_{fluide} \tilde{\tilde{W}}, \qquad (9)$$

with $\tilde{\tilde{Z}}_{fluide}(k_x, n) = \frac{\rho_0 \omega^2}{k_r} \frac{H_n^{(2)}(k_r R)}{H_n^{(2)\prime}(k_r R)}$, $k_r = \sqrt{{k_0}^2 - {k_x}^2}$,

and k_0, the acoustic wavenumber.

Introducing eq. (8) in eq. (6), one obtains a linear equation system which may be solved. Literal expressions for the spectral displacements $\tilde{\tilde{W}}, \tilde{\tilde{U}}, \tilde{\tilde{V}}$ and the spectral rotation, $\tilde{\tilde{\varphi}} = jk_x \tilde{\tilde{W}}$ are then obtained.

2.3.2 Circumferential admittance calculation

The circumferential admittances of the fluid loaded shell $Y^{\text{shell}}_{\xi_i \zeta_j}$ are estimated using the previous expression of the spectral displacement $\tilde{\tilde{\xi}}$ in the case of a line external load at x=0 with $\tilde{\zeta}_j = 1$.

A discrete field of the spectral displacement $\tilde{\tilde{\xi}}$ is obtained by discretizing and truncating the wavenumber space with adapted criterions such like those described in [11]. Inverse discrete Fourier transform on x-axis permit to have the spectral displacement $\tilde{\xi}_\zeta$ depending on x:

$$\tilde{\tilde{\xi}}_\zeta(k_x, n) \xrightarrow{I.F.T.} \tilde{\xi}_\zeta(x, k_\theta). \qquad (10)$$

The shell admittances $Y^{\text{shell}}_{\xi_i \zeta_j}$ are deduced by translating this result along x direction:

$$Y^{\text{shell}}_{\xi_i \zeta_j} = \tilde{\xi}_\zeta(x_i - x_j, k_\theta), \forall (i,j) \in ([1,\Theta])^2. \qquad (11)$$

In the case of an external load applied directly on the shell, the free displacements $\tilde{\tilde{\xi}}_i^{\text{shell}}$ may also be evaluated by this approach.

2.3.3 Numerical convergence improvement of the wave-number approach

The k_x convergence of the inverse Fourier transform of the spectral displacements could be more or less fast. It is very slow for the spectral rotation for an excitation by a moment, $\tilde{\tilde{\varphi}}_M$ (see the red curve in Fig. 4). It can be easily explained by its definitions: $\tilde{\tilde{\varphi}} = jk_x \tilde{\tilde{W}}$. To accelerate the k_x convergence, one proposes to consider the quantity Ω_M defined by:

$$\Omega_M(x,\theta) = \varphi_M(x,\theta) - \psi_M(x,\theta) \qquad (12)$$

where φ_M and ψ_M are both the rotation of the shell excited by the moment. For the first variable, φ_M the fluid loading are fully taken into account whereas for the second variable, ψ_M the fluid loading is approximated by its added mass effect.

Analytical expressions can be found for ψ_M and for its Fourier transform $\tilde{\psi}_M$. Then, by evaluating numerically the spectral quantity $\tilde{\tilde{\Omega}}_M$ and applying it the same process than in the previous section, one can estimate $\tilde{\Omega}_M$ without difficulty. Indeed, the k_x convergence of $\tilde{\tilde{\Omega}}_M$ is faster than the convergence of $\tilde{\tilde{\varphi}}_M$, as it is illustrated in Fig. 4.

One can finally deduce $\tilde{\varphi}_M$ with : $\tilde{\varphi}_M = \tilde{\Omega}_M + \tilde{\psi}_M$.

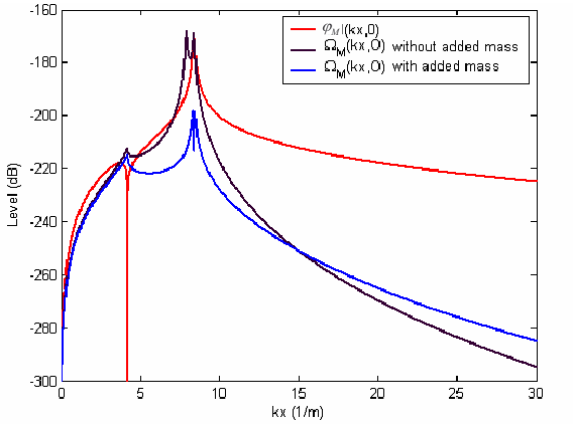

Figure 4. $\widetilde{\widetilde{\varphi}}_M(k_x,0)$ *and* $\widetilde{\widetilde{\Omega}}_M(k_x,0)$ *with/without added mass in* ψ_M.

2.4 Vibration and sound radiation from the fluid loaded shell coupled with its internal frames

From the forces/moments exerted by the frames on the shell, $\widetilde{\mathbf{F}}^{\mathbf{frame}}$ (see section 2.1) and using the developments of section 2.3.1, one calculates the spectral displacements of the shell coupled with its frames. With adapted criterions [11] and Inverse Discrete Fourier Transform, one deduces the displacement field in the physical space:

$$\widetilde{\widetilde{W}}(k_x,n) \xrightarrow{I.D.F.T.^2} W(x,\theta). \qquad (13)$$

The radiated pressure in the near field can be estimated with the same method whereas the radiated pressure in the far field can be estimated with the stationary phase theorem [10].

3 Numerical validations

The first test case consists in a periodically stiffened shell immersed in water (shell: radius 6.2 m, thickness 65 mm; stiffener: spacing 1.1 m, T-frame section 300mm x 60mm / 60mm x 300mm, material: steel).

The shell is excited by a radial point force at x_0 =0.3m, $\theta = 0°$. A reference result is given by an infinite periodic stiffened shell model whereas the CAA result is obtained by considering 40 stiffeners uniformly spaced and the excitation located between the 20th and 21st stiffeners. The comparison is given in Fig. 5 and shows a good agreement between the two models.

The second test case (see Fig. 6 (a)) consists in an *in vacuo* stiffened shell with a 100mm-thick bulkhead and clamped boundary conditions at its ends. Finite Element calculations with NASTRAN may be performed for this test case without external fluid. Comparisons with CAA are presented in Fig. 6 (b) and Fig. 6 (c) for a radial excitation and a longitudinal excitation, respectively. Results in term of radial and longitudinal displacements are almost identical between the two calculations. One can see that the bulkhead effect and the clamped boundary conditions are well taken into account by the circumferential admittance approach.

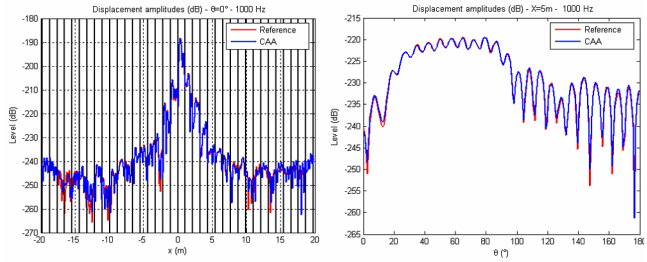

(a) *(b)*

Figure 5. Radial displacements for a periodically stiffened shell: (a), Results along the generator of the shell at $\theta = 0°$ *(black line: stiffener); (b), results along the circumference at x=5 m. Radial point force at* x_0*=0.3m,* $\theta = 0°$.

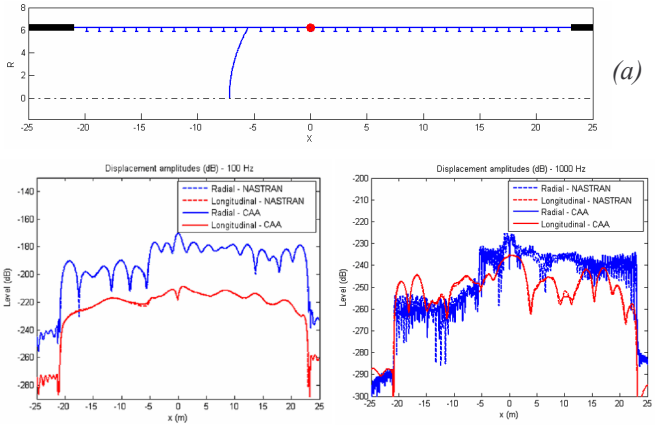

(a) *(b)* *(c)*

Figure 6. Second test case: (a), geometry; (b), radial and axial displacements at 100 Hz for a radial force at x=0m; (c), radial and axial displacements at 1000 Hz for an axial force at x=0m.

4 Vibration and radiation of a submarine hull

The submarine application case shown on Fig. 7 is composed of an 86m length and 45mm thick cylindrical shell stiffened with 97 stiffeners, 3 bulkheads and 2 stiffened ends caps. The stiffeners have different sections (four types of stiffeners) and their spacing varies from 0.7m to 1.1m. The shell is immerged in water and is excited by a radial point force on the web of the 52nd frame.

For the CAA calculation, we have introduced clamped boundary conditions at 2m away the ends of the shell in order to simulate the finite length of the shell (limitation of the wave propagations). An example of the radial acceleration in the wavenumber space $\widetilde{\widetilde{\gamma}}$ is given on Fig. 8. It is directly obtained from the coupling forces $\widetilde{\mathbf{F}}^{\mathbf{frame}}$ and the expression of the spectral displacement $\widetilde{\widetilde{W}}$ developed in section 2.3.1. Such result can help the understanding of the behaviour of the shell as it is proposed in reference [12] from measurements. Inverse discrete Fourier transforms of $\widetilde{\widetilde{\gamma}}$ give the acceleration in the real space as it is presented in Fig 9 (a) at 300 Hz. The associated radiated pressure in the far field and results for others frequencies are also presented on this figure. The computing times are given on Tab. 1. It should be noted that the calculation of the shell

admittance $\widetilde{Y}^{shell}_{\xi_i\zeta_j}$ should be achieved only one single time whatever the number of excitations. These results will be analyzed in a next paper.

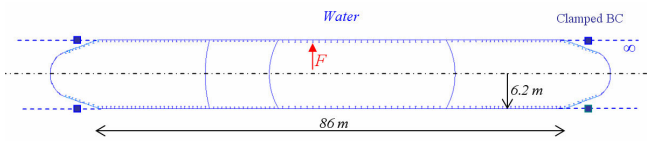

Figure 7. Submarine hull application case.

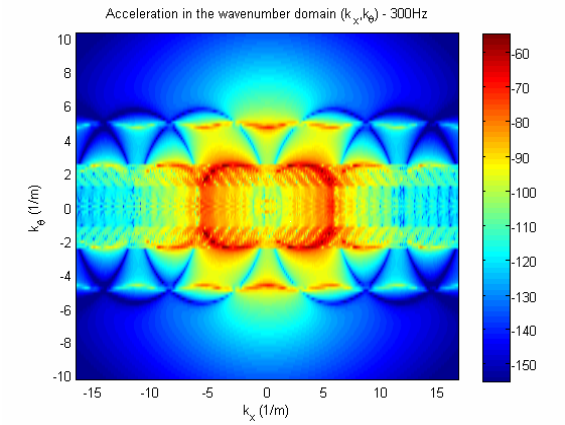

Figure 8. Acceleration in the wavenumber space - 300 Hz.

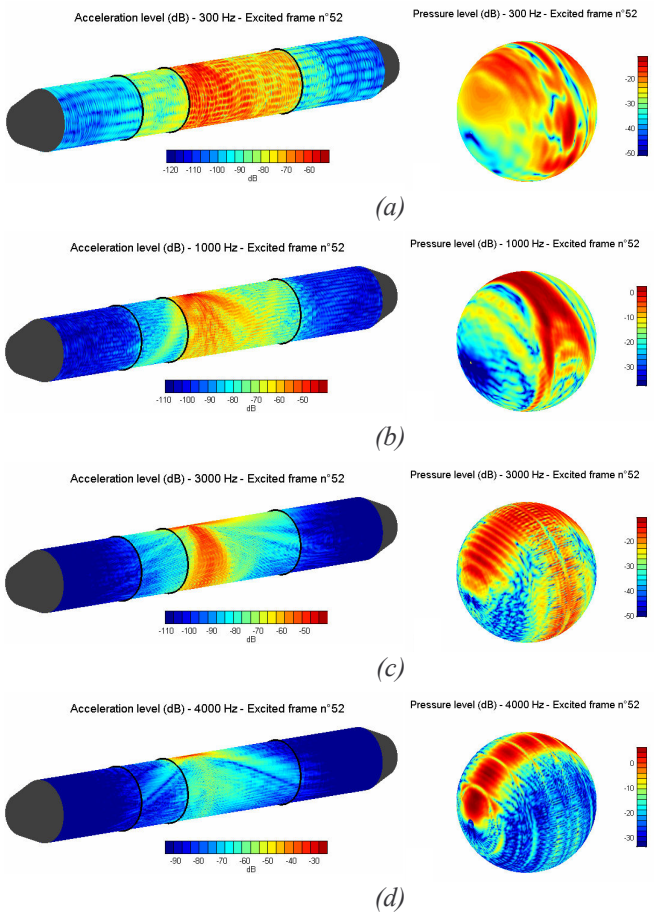

Figure 9. Levels of the radial acceleration of the shell (dB, ref. 1 m/s^{-2}) and the radiated pressure in the far field (dB, ref. 1 Pa.m): (a), 300 Hz ; (b), 1000 Hz ; (c), 3000 Hz ; (d), 4000 Hz.

	300 Hz	1000 Hz	3000 Hz	4000 Hz
$\widetilde{Y}^{shell}_{\xi_i\zeta_j}$	*70*	*111*	*212*	*250*
$\widetilde{\mathbf{F}}^{frame}$	*16*	*26*	*48*	*54*
$\widetilde{\widetilde{W}}$	*16*	*29*	*84*	*112*
IDFT^2	*2*	*4*	*15*	*20*
Total	***104***	***170***	***359***	***436***

Table 1. CPU time (sec.) PC Pentium IV 3GHz

5 Conclusions

CAA is a powerful tool to assemble analytical model of a shell with FE models of its internal frames. With reasonable computing time, it permits to evaluate the vibratory field of a submarine pressure hull and its radiated pressure field, as well as in the near field than in the far field. Mechanical and acoustic loads may be considered for these calculations. The intermediary results of this approach which are the displacements and the pressures expressed in the wavenumber space are interesting to analyse the behaviour of the shell. In the future, this technique will be extended to non- axisymmetric internal frames.

6 Reference

[1] Zampolli, M., Tesei A., Jensen, F.B., Malm, N., Blottman III, J.B. – A computationally efficient finite element model with perfectly matched layers applied to scattering from axially symmetric objects. JASA, Vol. 122, n°3, p.1472-1485, 2007.

[2] Yan J., Li T.Y., Liu T.G., Liu J.X., Characteristics of the vibrational power flow propagation in a submerged periodic ring-stiffened cylindrical shell, Applied acoustics, Vol. 67, p. 550-569, 2006.

[3] Yan J., Li T.Y., Liu J.X., Zhu X., Space harmonic analysis of sound radiation from a submerged periodic ring-stiffened cylindrical shell, Applied acoustics, Vol. 67, p. 743-755, 2006.

[4] Zhang W., Vlahopoulos N., Wu K., An energy finite element formulation for high-frequency vibration analysis of externally fluid-loaded cylindrical shells with periodic circumferential sitffeners subjected to axi-symmetric excitation. JSV, Vol. 282, p.679-700, 2005.

[5] Marcus M. H., Houston B.H., Photiadis D.M., Wave localization on a submerged cylindrical shell with rib aperiodicity. JASA, Vol. 109, n°3, p.865-869, 2001.

[6] Marcus M. H., Houston B.H., Energy pass bands in a ribbed cylindrical shell with periodic asymmetries. JASA, Vol. 118, n°4, p.2167-2172, 2005.

[7] Liétard, R, Décultot, D., Maze G., Tran-Van-Nhieu, M. - Acoustic scattering from a finite cylindrical shell with evenly spaced stiffeners : Experimental investigation. JASA, Vol. 118, n°4, p.2142-2146, 2005.

[8] Zhou, Q., Joseph, P.F. – A numerical method for the calculation of dynamic response and acoustic radiation from an underwater structure. JSV, Vol. 283, p.853-873, 2005.

[9] Karczub, D.G. – Expressions for direct evaluation of wave number in cylindrical shell vibration studies using the Flügge equations of motion. JASA, n°119 (6), p. 3553- 3557, 2006.

[10] Junger M.C.and Feit, D. *Sound, Structures and Their Interaction*, The MIT press, Cambrige, Second edition, 1986. 448 p.

[11] Maxit, L., Vibration and acoustic radiation analysis of a stiffened fluid-loaded plate using a wavenumber approach and a discrete Fourier transform. In: 19th International Congress on Acoustics 2007 – Madrid, Spain, September 2007.

[12] Photiadis, D.M., Williams, E.G., Houston, B.H. – Wave-number space response of a near periodically ribbed shell. JASA, n°101 (2), p. 877-886, 1996.